ChemPubSoc Europe

DOI: 10.1002/chem.201404216

CHEMISTRY A European Journal Full Paper

Supramolecular Chemistry

Multistimuli-Responsive Supramolecular Assembly of Cucurbituril/Cyclodextrin Pairs with an Azobenzene-Containing Bispyridinium Guest

Jin Zhao, Ying-Ming Zhang, He-Lue Sun, Xiao-Yu Chang, and Yu Liu*[a]

Abstract: A linear supramolecular architecture was successfully constructed by the inclusion complexation of α-cyclodextrin with azobenzene and the host-stabilized charge-transfer interaction of naphthalene and a bispyridinium guest with cucurbit[8]uril in water, which was comprehensively characterized by ^{1}H NMR spectroscopy, UV/Vis absorption, fluorescence, circular dichroism spectroscopy, dynamic laser scattering, and microscopic observations. Significantly, because it benefits from the photoinduced isomerization of the azophenyl group and the chemical reduction of bispyridinium moiety with noncovalent connections, the assembly/disassembly process of this supramolecular nanostructure can be efficiently modulated by external stimuli, including temperature, UV and visible-light irradiation, and chemical redox.

Introduction

Reversibly switchable supramolecular architectures with well-defined nanostructures are of great importance owing to their unique properties and immense potential applications in various fields.[1] The dynamic reversibility of noncovalent interactions and the incorporation of stimuli-switchable components into building blocks can endow these nanostructures with responsive capability to various external triggers, such as pH,[2] temperature,[3] photoirradiation,[4] and (electro)chemical redox.[5] Among these nanosupramolecular assemblies, a supramolecular polymer, a one-dimensional nanoarray constructed by incorporating multiple small-molecular-weight monomers into the linear polymeric framework, has attracted special attention, as they can combine the advantages of polymer and supramolecular chemistry and confer practical superiority on controlled drug-delivery systems, molecular machines, and optoelectronic materials.[6]

In this context, it is noteworthy that the efficient integration of two or several different types of macrocycles into a single supramolecular assembled entity has been proven to be an alternative and an even more powerful strategy to fabricate advanced multistimuli-responsive nanomaterials, because the different macrocyclic receptors might possess mutual complementarity in molecular-binding selectivity.[7] Taking two representative macrocycles, cyclodextrin (CD) and cucurbituril (CB), as an example, the former can be functionalized to encapsulate various neutral and negatively charged substrates in their hydrophobic microenvironments, mainly through the hydrophobic interaction, whereas the latter is prone to entrap the positively charged aromatic conjugates and cationic complexes mainly through ion–dipole interactions. Consequently, considerable effort has been devoted to exploring the macrocycle-based supramolecular polymers and hetero-polyrotaxanes with fascinating multistimuli-responsive characteristics. For instance, Zhang and co-workers have fabricated a supramolecular polymer based on the self-sorting of CB[7]- and CB[8]-containing complexes, in which the molecular weight could be conveniently controlled by tuning the content of CB[7].[8] Moreover, Li and Tian et al. have reported a linear supramolecular assembly with helical chirality from the molecular recognition of α-CD and calix[4]arene, and the morphology of such a supramolecular polymer could be tailored by the incorporation of a photoresponsive azobenzene molecule.[7c]

Inspired by these promising results and as a part of our ongoing program on the construction of multicomponent supramolecular assemblies, herein we report the fabrication of a multistimuli-responsive supramolecular assembly based on naphthalene-modified α-CD, CB[8], and azobenzene-containing bispyridinium salt. By benefiting from the specific molecular binding of *trans*-azobenzene with α-CD and a host-enhanced charge-transfer complex between naphthalene and a bispyridinium salt, it was found that α-CD and CB[8] can be aligned in a linear arrangement and is mediated by the equidistant and regular host–guest complexation in aqueous media. More importantly, as investigated by the spectroscopic experiments, the noncovalent interactions in this linear assembly are inherently susceptible to the external signals, that is, the photoin-

[a] J. Zhao, Dr. Y.-M. Zhang, H.-L. Sun, X.-Y. Chang, Prof. Dr. Y. Liu
Department of Chemistry, State Key Laboratory of
Elemento-Organic Chemistry, Collaborative Innovation Center
of Chemical Science and Engineering (Tianjin)
Nankai University, Tianjin 300071 (P.R. China)
E-mail: yuliu@nankai.edu.cn

Supporting information for this article is available on the WWW under http://dx.doi.org/10.1002/chem.201404216. It includes detailed experimental procedures, characterization of compounds **1** and **2**, additional 2D NMR, ESI-MS, UV/Vis, fluorescence, and circular dichroism spectra, Job plots, microscopic images, as well as ITC curves.

duced isomerization of the azobenzene unit, the chemical reduction of the bispyridinium moiety, and the temperature-sensitive assembly and disassembly process upon heating and cooling treatment. Therefore, the present system could be considered a promising strategy for attaining a multistimuli-responsive supramolecular assembly at a molecular level.[9]

Results and Discussion

Synthesis and conformational analysis

The naphthalene-modified α-CD (**1**) was synthesized through the 'click' reaction of 6-deoxy-6-azido-α-CD with 2-hydroxyl-6-propargyloxy naphthalene.[10] The azobenzene–bispyridinium conjugate (**2**) was obtained from the brominated azobenzene and 1-methyl-4-(4-pyridyl)pyridinium iodide in a moderate yield (Scheme S1 and Figures S1–S8 in the Supporting Information). All the characteristic ^{1}H resonances in compounds **1** and **2** were clearly assigned by the use of 2D NMR correlation spectroscopy (COSY) in D_2O (Figures S9–S13 in the Supporting Information). As shown in the ^{1}H NMR spectra of **1** in [D_6]DMSO, the peak pattern in the region of $\delta = 7.03$–9.48 ppm, which corresponds to the aromatic protons of triazole and naphthyl groups, was quite similar to the one recorded in D_2O, thereby suggesting that the naphthyl moiety was not self-included in the CD cavity (Figure S14 in the Supporting Information). Then, the precise structural information of **1** was directly obtained by rotating-frame Overhauser effect spectroscopy (ROESY) experiments in aqueous solution, in which no clear Overhauser enhancement (NOE) correlation was found between the protons of the naphthyl substituent and the interior protons of the CD (Figure S15 in the Supporting Information). This phenomenon further confirms that the CD cavity was unoccupied in compound **1**, and more importantly, this molecular conformation would facilitate the complexation of the azophenyl unit in **2** with the α-CD cavity, as described below. The molecular structures and proton designation of compounds **1**, **2**, CB[8], and reference **3** are shown in Scheme 1.

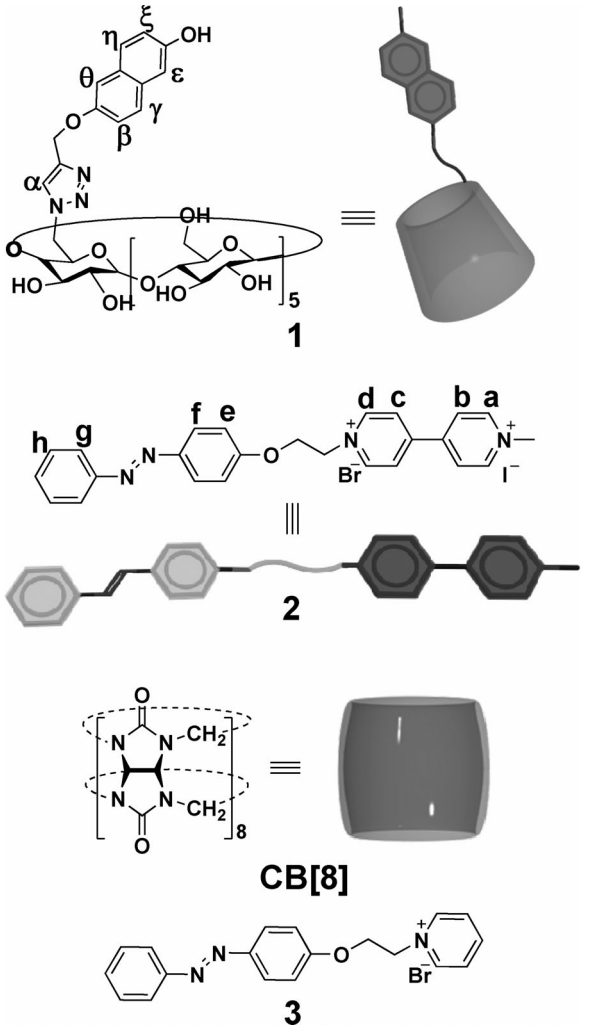

Scheme 1. Molecular structures and proton designation of compounds **1**, **2**, CB[8], and reference **3**.

^{1}H NMR spectroscopic titration

The formation of supramolecular complex **1·2** was preliminarily investigated by means of ^{1}H NMR spectroscopy. For comparative purposes, the chemical-shift changes ($\Delta\delta$) for all of the examined complexes are listed in Table S1 in the Supporting Information. As shown in Figure 1, the protons of the naphthyl group in **1** underwent a pronounced upfield shift upon addition of **2** ($\Delta\delta_{\beta,\mathbf{1\cdot2}} = -0.22$ ppm, $\Delta\delta_{\gamma,\mathbf{1\cdot2}} = -0.37$ ppm, and $\Delta\delta_{\varepsilon,\mathbf{1\cdot2}} = -0.58$ ppm), whereas those of the azophenyl group ($H_{e,g,h}$) in **2** gave a complex-induced downfield shift ($\Delta\delta_{e,\mathbf{1\cdot2}} = 0.18$ ppm, $\Delta\delta_{g,\mathbf{1\cdot2}} = 0.36$ ppm, and $\Delta\delta_{h,\mathbf{1\cdot2}} = 0.06$ ppm). Furthermore, the cross-peaks between the azophenyl moiety and CD cavity were clearly observed in the ROESY spectrum of the **1·2** complex (Figure S16 in the Supporting Information). These observations indicate that the *trans*-azobenzene group of **2** can be encapsulated in the cavity of **1**, which arises from the high affinity with α-CD, thus leaving the bispyridinium moiety outside the CD cavity. Comparatively, when CB[8] was added into the solution of the **1·2** complex, it was found that the NMR spectroscopic signals of naphthyl in **1** and the bispyridinium group in **2** (H_{a-d}) were shifted upfield, whereas those of the azobenzene group in **2** ($H_{e,f}$) showed a downfield shift.

Furthermore, it can be seen that both the bispyridinium ($H_{b,c}$) and azophenyl ($H_{e,f}$) proton signals were shifted upfield ($\Delta\delta_{b,\mathbf{2}\cdot CB[8]} = -1.54$ ppm, $\Delta\delta_{c,\mathbf{2}\cdot CB[8]} = -1.48$ ppm, $\Delta\delta_{e,\mathbf{2}\cdot CB[8]} = -1.19$ ppm, and $\Delta\delta_{f,\mathbf{2}\cdot CB[8]} = -0.70$ ppm), whereas there was also a moderate downfield shift for $H_{g,h}$ ($\Delta\delta_{g,\mathbf{2}\cdot CB[8]} = 0.08$ ppm and $\Delta\delta_{h,\mathbf{2}\cdot CB[8]} = 0.09$ ppm) upon addition of CB[8] to the solution of **2** (Figure 1d and e). These different variations in the $\Delta\delta$ values of aromatic protons demonstrate that CB[8] moves rapidly between the bispyridinium and azobenzene terminals. In addition, the peak at *m/z* 862 was assigned to $[\mathbf{2}+CB[8]-I-Br]^{2+}$ (Figure S20 in the Supporting Information). In addition, after adding **1** to the **2**·CB[8] complex at an equivalent molar ratio, the ^{1}H NMR spectrum of the **2**·CB[8]·**1** complex was obtained, which resembled that of the **1·2**·CB[8] complex, thus suggesting that the addition sequence cannot affect the spontaneous formation of the ternary complex (Figure 1c).

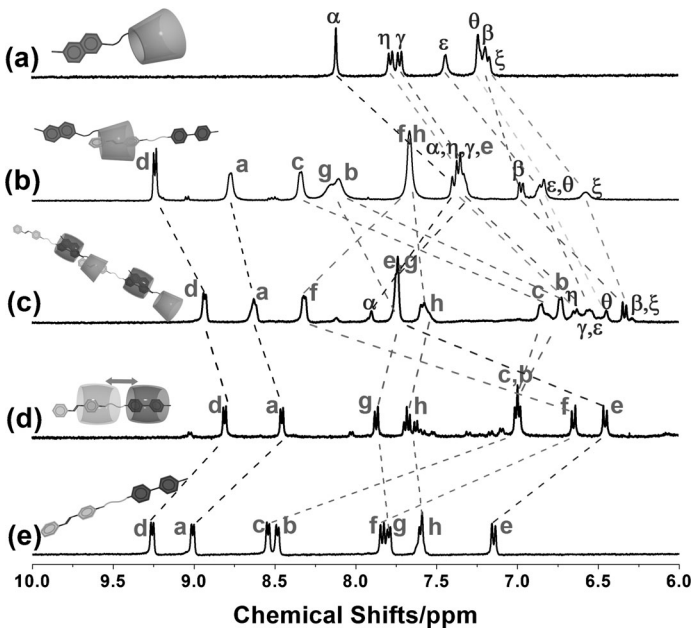

Figure 1. ^{1}H NMR spectra of a) **1**, b) **1·2** complex, c) **1·2**·CB[8] complex, d) **2**·CB[8] complex, and e) **2** in D_2O at 25 °C, respectively (400 MHz, [**1**] = [**2**] = [CB[8]] = 2.0 mM).

Moreover, as seen from Figure S17 in the Supporting Information, the NOE correlation between the naphthalene and bispyridinium moiety could be found, thus suggesting that CB[8] as a molecular connector can concurrently entrap the electron-deficient bispyridinium salt and electron-rich naphthalene to form **1·2**·CB[8] complex (peak A in Figure S17). The NOE cross-peaks between the protons of CB[8] and α-CD (H2 and H3) were also observed, thus suggesting that these two macrocycles were located closely to each other (peak B in Figure S17). Meanwhile, the NOE correlation peaks between the azobenzene and α-CD indicate that the introduction of CB[8] cannot make any negative impact on the inclusion complexation of azobenzene with α-CD (peaks C in Figure S17 in the Supporting Information).[11] In addition, this selective binding process was further evidenced by mass spectrometry, in which the peaks at *m/z* 795 and 1460 could be clearly assigned to the complexes of $[\mathbf{1}+\mathbf{2}-\mathrm{I}-\mathrm{Br}]^{2+}$ and $[\mathbf{1}+\mathbf{2}+\mathrm{CB[8]}-\mathrm{I}-\mathrm{Br}]^{2+}$, respectively (Figures S18 and S19 of the Supporting Information).

UV/Vis and circular dichroism spectroscopy

To further investigate the molecular binding mode in the formation of the supramolecular assembly, UV/Vis and fluorescence spectroscopic experiments were carried out in water. As discerned from Figure 2b, at lower concentration, two characteristic absorption bands at 340 and 430 nm that originated from π–π* and n–π* transitions of the azophenyl unit in **2** were dramatically enhanced upon complexation with α-CD,[12] accompanied by the bathochromic shifts of 6 and 11 nm, respectively. It is well known that the molecular binding of CB[8] with the donor and acceptor chromophores can induce a remarkable change in the long-wavelength region.[11,13] In our case, there was no absorption beyond 550 nm for the individual compound of **1** or **2**, or the equimolar mixture of **1·2** or **2**·CB[8] at higher concentration, whereas a new broad absorption that ranged from 520 to 700 nm was observed in the **1·2**·CB[8] complex, thus substantiating the CB[8]-enhanced charge-transfer (CT) interaction between the electron-donating naphthyl moiety and the electron-accepting bispyridinium unit (Figure 3). In addition, the emission intensity of naphthalene in the **1·2**·CB[8] complex was quenched by 57% relative to the **1·2** complex, mainly on account of the noncovalent binding with CB[8] that can draw the naphthyl and bispyridinium groups much closer in its cavity (Figure S21 in the Supporting Information). Moreover, as seen in Figure S22 in the Supporting Information, a similar CT band in the range of 520 to 700 nm was observed by simply mixing the **2**·CB[8] complex with 6-methoxy-2-naphthol as reference, thus demonstrating that the CT interaction originated from the complexation of CB[8] with the naphthyl group in **1** and the bispyridinium group in **2**.

Moreover, as depicted in Figure 2a, the equimolar mixture of **1** and **2** exhibited positively and negative-

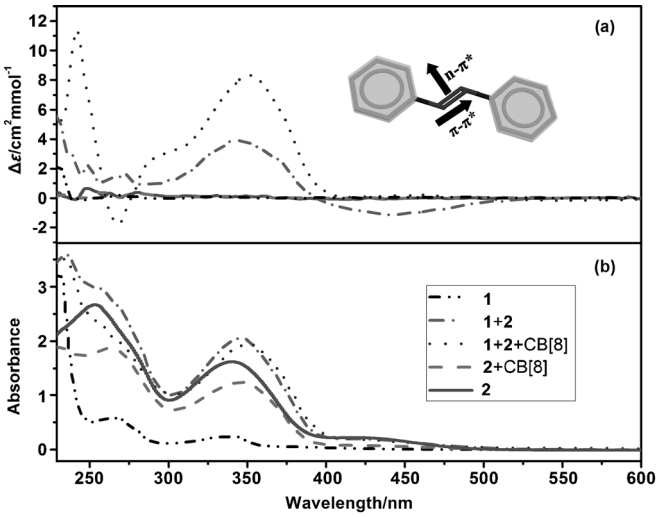

Figure 2. a) Circular dichroism and b) UV/Vis absorption spectra of **1**, **2**, **1·2** complex, **2**·CB[8] complex, and **1·2**·CB[8] complex, respectively, in water at 25 °C ([**1**] = [**2**] = [CB[8]] = 0.1 mM).

ly induced circular dichroism (ICD) signals in the π–π* and n–π* absorption regions of azobenzene, respectively. According to the ICD empirical rules on the CD-based complexes,[14] and by combining the aforementioned 2D NMR spectroscopic results, we can reasonably infer that the azophenyl moiety in **2** was incorporated along the axial direction of the CD cavity in **1**. When CB[8] was added, a new CD Cotton effect peak was observed in the range from 228 to 278 nm for the ternary complex of **1·2**·CB[8], which might reflect the coupled interaction between the naphthyl and bispyridinium groups in the CB[8] cavity.[15] In addition, the enhanced positive band for the azobenzene π–π* transition in the presence of **1** here again re-

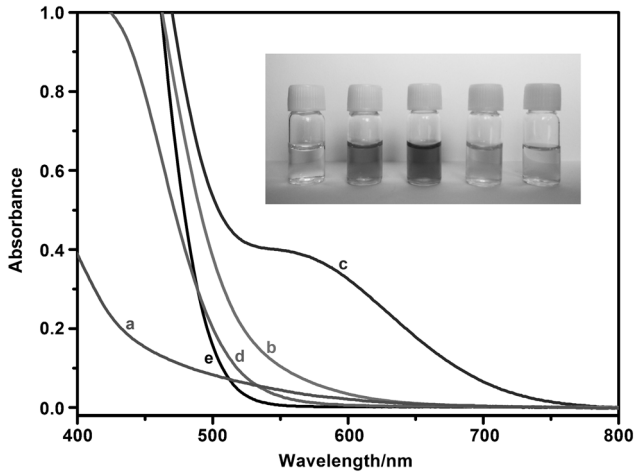

Figure 3. UV/Vis absorption spectra of a) **1**, b) **1·2** complex, c) **1·2**·CB[8] complex, d) **2**·CB[8] complex, and e) **2** in water at 25 °C in the range from 400 to 800 nm to comparatively show the CT band at higher concentration ([**1**] = [**2**] = [CB[8]] = 1.0 mM). Inset: Visible color changes of **1**, **1·2** complex, **1·2**·CB[8] complex, **2**·CB[8] complex, and **2**, respectively (from left to right).

veals the encapsulation of the azophenyl unit inside the CD cavity.[14] It is noteworthy that the host–guest interaction in these supramolecular complexes could be readily distinguished not only by the spectroscopic titration but also the color change of the resultant solution; that is, compound **1** or **2** alone was colorless or light yellow but turned orange and brown in the presence of **1** and CB[8] (inset photos in Figure 3). Overall, these spectral changes jointly demonstrate the formation of a ternary **1·2**·CB[8] complex, which was constructed by the noncovalent complexation with α-CD and CB[8] pairs in aqueous solution.

Determination of binding constants

First, the Job plots of **1·2**, **2**·CB[8], and **1·2**·CB[8] complexes were carried out to investigate the inclusion behaviors; they gave a 1:1 complex stoichiometry in all cases (Figures S23–S25 in the Supporting Information). Then, to quantitatively investigate the molecular binding behaviors and thermodynamic control factors in these obtained complexes, isothermal titration calorimetry (ITC) experiments were performed in phosphate buffer (pH 7.2). In our case, the azophenyl derivative (**3**) that bore a pyridinium substituent was selected as the model molecule. As seen from Figures S26 and S27 in the Supporting Information, the microcalorimetric titration experiments gave a typical curve for 1:1 complexation between the CD cavity of **1** and the *trans*-azobenzene group of **3** with a binding constant of $1.02\times10^{4}\,M^{-1}$ (Table S2 in the Supporting Information). This complexation process was driven by a favorable enthalpy change ($\Delta H^{\circ} = -39.37\ kJ\,mol^{-1}$), accompanied by a negative entropy change ($T\Delta S^{\circ} = -16.48\ kJ\,mol^{-1}$). Similarly, the binding ability of the charge-transfer complex of the **1·2** complex with CB[8] can be simplified by using methyl viologen (MV^{2+}) as model molecule. The naphthyl group of **1** can efficiently bind MV^{2+}·CB[8] complex, which was governed in a thermodynamically favorable way with a stability constant of $6.52\times10^{5}\,M^{-1}$ (Figures S28 and S29 in the Supporting Information).

Characterization of the supramolecular assembly

Dynamic light scattering (DLS), diffusion-ordered spectroscopy (DOSY), and viscosity measurements were performed to provide evidence for the formation of the supramolecular assembly in solution. As shown in Figure 4a, two hydrodynamic diameter distributions of **1·2**·CB[8] were detected, in which one centered at 14 nm could be ascribed to the low-molecular-weight assembly and the other one centered at 97 nm was assigned to the large-sized supramolecular aggregation. In DOSY experiments, relative to the diffusion coefficient of the **2**·CB[8] complex ($2.07\times10^{-10}\,m^{2}\,s^{-1}$), the corresponding value of the **1·2**·CB[8] assembly was relatively lower ($1.46\times10^{-10}\,m^{2}\,s^{-1}$)

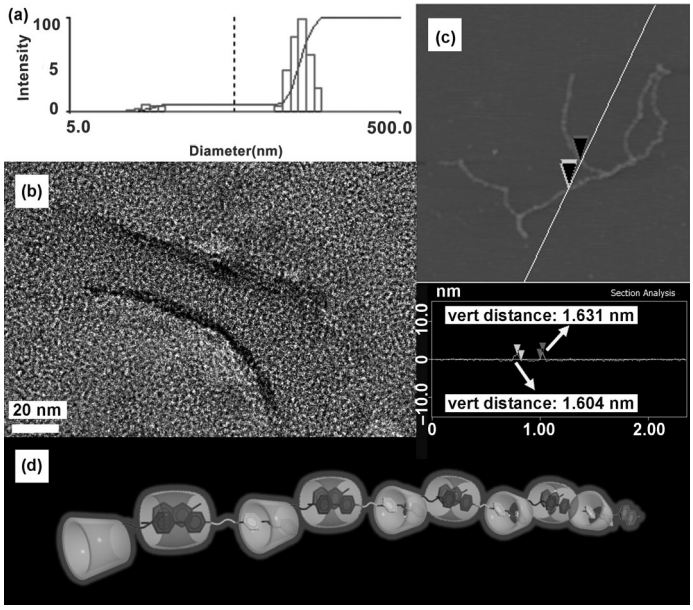

Figure 4. a) Diameter distributions of **1·2**·CB[8] assembly (0.1 mM) in water at 25 °C; b) TEM and c) AFM images, and d) schematic representation of the **1·2**·CB[8] assembly.

under the same experimental conditions, thereby substantiating that the resultant assembly can diffuse as one entity with a higher molecular weight (Figures S31 and S32 in the Supporting Information). Moreover, in the logarithmic plot of the specific viscosity versus the concentration of **1·2**·CB[8], a gradual increase for the predominance of the resulting assembly was observed with a clear inflection point at 0.6 mM as the critical aggregation concentration, above which the monomers could be exclusively transferred to a highly ordered supramolecular assembly (Figure S33 in the Supporting Information). These obtained results jointly support the formation of a supramolecular assembly **1·2**·CB[8] in water.

Furthermore, the morphological information on the size and shape of assembly **1·2·**CB[8] was characterized by transmission electron microscopy (TEM) and atomic force microscopy (AFM). Along with the formation of the **1·2·**CB[8] supramolecular assembly in solution, Figure 4b shows that a 1D linear morphology was observed in the TEM image with the length and width of approximately 100 and 1.7 nm, respectively. As shown in Figure 4c, similar linear objects were also found in the AFM images and the height of these 1D nanostructures was 1.6 nm, which was consistent with the average size of the diameter of α-CD and CB[8]. In addition, it can be seen that these linear assemblies were cross-linked with each other mainly through the intermolecular hydrogen-bonding interconnection of the hydroxyl groups in the α-CD skeleton.[16]

To gain more insight into the molecular binding mode of **1** and **2** with CB[8], some control experiments were performed. Apart from the naphthyl groups, it has been reported that the azobenzene derivatives also have a tendency to form a CB[8]-assisted multicomponent complex,[17] and theoretically, an *n*:*n* type of linear supramolecular polymer can be expected in the equimolar mixture of azobenzene–bispyridinium conjugate **2** and CB[8] (Scheme S2 in the Supporting Information). However, no large aggregation was observed in DLS and viscosity measurements (Figures S30 and S33 in the Supporting Information). Furthermore, by comparing the diffusion coefficients of **2·**CB[8] with MV^{2+}·CB[8] complexes, it can be deduced that the average size of the **2·**CB[8] complex was only 3.3 times larger than the one of the MV^{2+}·CB[8] complex (see the Supporting Information). Therefore, the one-dimensional wirelike aggregation based on the binary **2·**CB[8] complex can be reasonably excluded in our case. This phenomenon is mainly attributed to the naphthyl group in **1**, which, relative to azobenzene, is a better candidate to form a stable charge-transfer complex with the electron-deficient salt inside the CB[8] cavity. In addition to the strong binding affinity of naphthalene and bispyridinium with CB[8], the high orientation selectivity that originates from the multiple hydrophobic and charge-transfer interactions is considered to be another basic and crucial factor to facilitate the formation of the supramolecular polymer **1·2·**CB[8].[18]

Multistimuli-response of the supramolecular assembly

Since the stimuli-responsive groups of azobenzene and bispyridinium moieties were incorporated as the building blocks, the obtained supramolecular assembly **1·2·**CB[8] has the ability to respond to external triggers (i.e., temperature, photoirradiation, and redox). As shown in Figure 5, the absorbance at 351 nm of the supramolecular assembly decreased gradually with temperature ascending from 10 to 60 °C, thus corroborating that the azobenzene was expelled from the α-CD cavity. In contrast, the absorbance at 351 nm was slightly changed for the individual compounds **1** and **2** under the same experimental conditions (Figures S34 and S35 in the Supporting Information). On the contrary, when the same sample was cooled from 60 to 10 °C, the stronger absorption strength for a **1·2·**CB[8] assembly was reproduced, which is indicative of the recombination of **1**, **2**, and CB[8] to form the linear assembly. The reversible spectral change was also observed from the circular dichroism spectra, in which the strength of a positive ICD peak at 351 nm was very sensitive to the temperature change over a wide range from 10 to 80 °C (Figures S36–S38 in the Supporting Information).

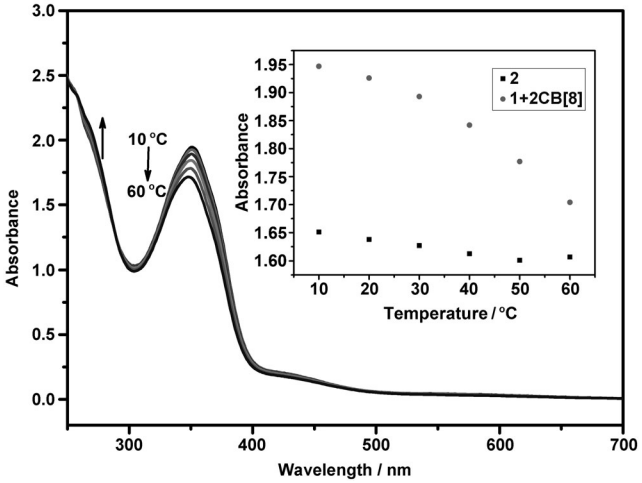

Figure 5. UV/Vis absorption spectra of the **1·2·**CB[8] assembly observed at different temperatures. Inset: Dependence of the absorbance of **2** and **1·2·**CB[8] assembly at 350 nm on temperature.

Apart from the α-CD/azobenzene complex, it is known that the stability of the CB-stabilized multicomponent complex can be decreased upon heating in solution, ultimately resulting in the disassociation of these supramolecular complexes.[19] In our case, the naphthyl group was excluded from the cavity of CB[8], as identified by the UV/Vis and circular dichroism spectroscopic investigation. The amplitude of the CD curves at 250 nm and the absorbance at 270 nm gave the reversible changes in the heating/cooling cycles (Figure 5 and Figure S38 in the Supporting Information). It is noted that this assembly/disassembly conversion can be repeatedly modulated several times (Figure 6). To summarize the above results, the two noncovalent interactions, host–guest interaction, and host-stabilized charge-transfer interaction are all susceptible to the thermal stimulus, which can be used in tuning the formation of the resultant assembly.

Owing to their superior photochemical properties, the photochromic azobenzene derivatives can exhibit the reversible photoisomerization between *trans* and *cis* isomers by UV- and visible-light irradiation. In the case of compound **2**, the π–π* transition absorption at 340 nm was dramatically decreased and the n–π* transition absorption at 430 nm was accordingly increased upon irradiation at 365 nm, thus indicating the transformation from the *trans*- to the *cis*-azobenzene in **2** (Figure 7a and Figure S39 in the Supporting Information). Consequently, the **1·2·**CB[8] assembly can be disrupted upon UV irradiation, because the binding affinity between *cis*-azobenzene and α-CD is rather lower than the *trans* isomer.[12] Under further irradiation at 450 nm, the dissembled components could be rearranged and switched to a large aggregation with good reversibility as soon as the *trans*-azobenzene was accommodated in

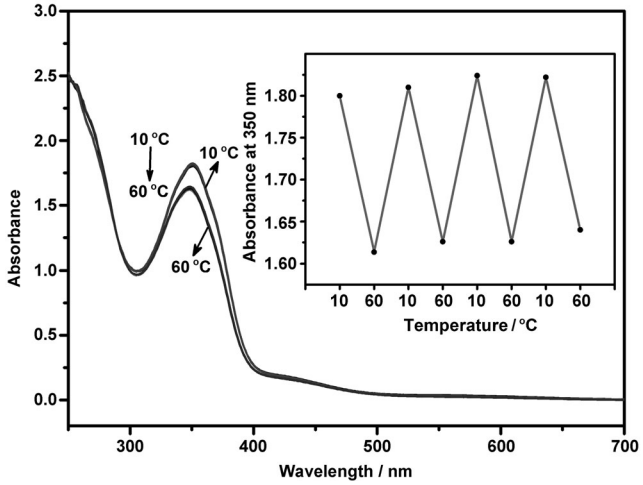

Figure 6. UV/Vis absorption spectra of the **1·2**·CB[8] assembly observed upon several cycles of thermal equilibration at 10 and 60 °C. Inset: Absorbance changes at 350 nm.

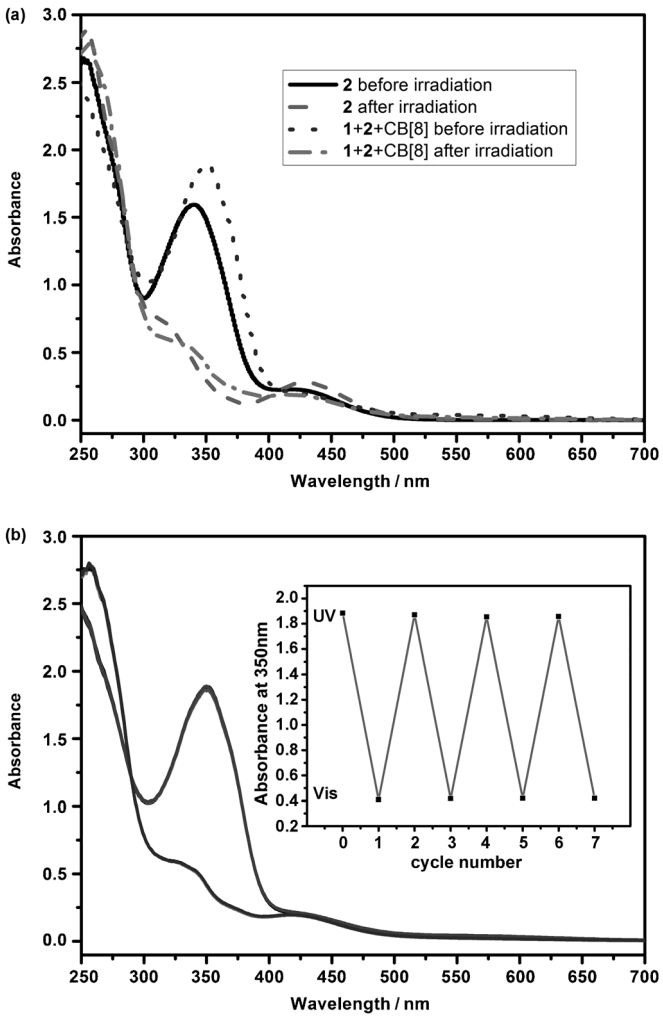

Figure 7. a) Photoisomerization process of **2** and the **1·2**·CB[8] assembly before and after UV irradiation. b) UV/Vis absorption spectra of the **1·2**·CB[8] assembly upon alternating UV- and visible-light irradiation in water. Inset: Absorbance changes at 350 nm ([**1**] = [**2**] = [CB[8]] = 0.1 mM).

the α-CD cavity (Figure 7b and Figure S40 in the Supporting Information). Moreover, as shown in Figure S41b of the Supporting Information, some new peaks could be observed in the NMR spectrum of the **1·2**·CB[8] complex after UV irradiation, which originated from the photoisomerization of the azophenyl group. Meanwhile, when the **1·2**·CB[8] assembly was exposed to UV irradiation, a hydrodynamic diameter centered at 155 nm was observed, and some spherical objects could be detected in the TEM and AFM experiments. It can be speculated that the photoisomerization of azobenzene was able to induce the dissociation of the **1·2**·CB[8] assembly to the **1**·*cis*-**2**·CB[8] complex. The latter complex was composed of a *cis*-azobenzene as the hydrophobic group and a cyclodextrin as the hydrophilic group, which had a tendency to form an amphipathic assembly (Figures S42–S44 in the Supporting Information).

It is well documented that a bispyridinium salt can be readily transformed to the corresponding radical-cation and neutral states by either chemical or electrochemical reduction methods. As expected, after treatment of **2** with sodium dithionite ($Na_2S_2O_4$) as a reducing agent, the remarkable changes in the UV/Vis spectra and the color of the solution were observed. As shown in Figure 8, the appearance of new absorption bands

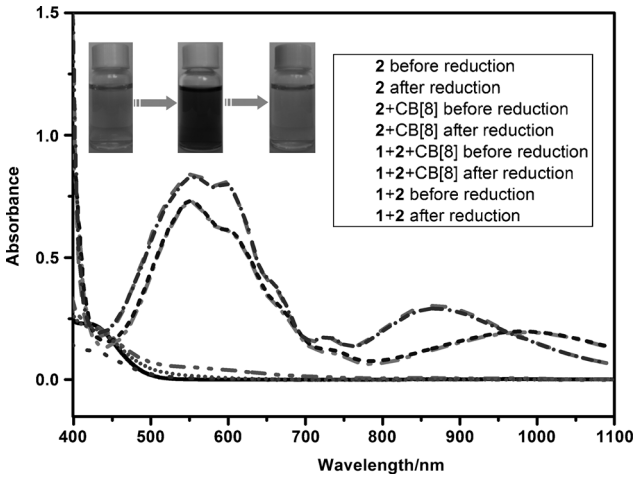

Figure 8. UV/Vis absorption spectra of **2**, **1·2**, **2**·CB[8], and **1·2**·CB[8] before and after reduction by an excess amount of $Na_2S_2O_4$. Inset: Visible color changes of **1·2**·CB[8] assembly after reduction by $Na_2S_2O_4$ and then oxidization by O_2 (from left to right).

from 450 to 1100 nm were caused by the transformation from dications to the radical cations of the bispyridinium moiety in **2**. Moreover, a similar UV/Vis spectral change was observed in the case of the **1·2** complex, thus indicating that the complexation of azobenzene with α-CD cannot influence the radical-cation formation of **2**. In contrast, the reduction of the **1·2**·CB[8] assembly gave rise to a strikingly different spectrum with the absorption maxima at 551 and 981 nm, which resembled that of the **2**·CB[8] complex in the long-wavelength region. These phenomena imply the formation of the $(\mathbf{2}^{+\bullet})_2$·CB[8] complex, in which the radical-cation dimers of **2** were simultaneously located in the CB[8] cavity.[11a,20] Since CB[8] can

efficiently stabilize the radical cations of bispyridinium, the $(\mathbf{2}^{+\bullet})_2$·CB[8] complex could remain stable in aqueous solution for several hours without any color change (Figure 8, inset). Moreover, owing to the oxygen-sensitive property of bispyridinium radical cations, the introduction of O_2 into the reduced solution would regenerate the bispyridinium dication and then lead to the formation of a supramolecular assembly. Along with the UV/Vis spectroscopic results, the NMR spectrum of the **1**·**2**·CB[8] complex showed that the peaks assigned to component **2** completely disappeared after reduction with an excess amount of $Na_2S_2O_4$, mainly on account of the paramagnetism of bispyridinium radical cations (Figure S41c in the Supporting Information). The DLS data of the **1**·**2**·CB[8] assembly also showed a main hydrodynamic diameter centered at 321 nm after reduction, which might be attributed to the undesirable cross-linking between the carbonyl-group portals of CB[8] and the excess amount of Na^+ in water. Accordingly, only amorphous morphological structures could be observed in the TEM and AFM images, convincingly proving the dissociation of the **1**·**2**·CB[8] linear assembly under the chemical reduction conditions (Figure S45 and S46 in the Supporting Information).

Conclusion

In conclusion, we have reported the construction of a linear assembly based on two kinds of macrocyclic receptors (α-CD and CB[8]) as hosts and the azobenzene–bispyridinium conjugate as guest in aqueous media. The formation of this multicomponent assembly was driven by the combination of the host–guest inclusion complex of α-CD with *trans*-azobenzene and the CB[8]-assisted charge-transfer complex between naphthalene and a bispyridinium salt. More interestingly, as demonstrated by the spectroscopic and microscopic investigations, this supramolecular nanoarchitecture could be efficiently modulated in a controlled manner by multiple external stimuli, including temperature, light irradiation, and redox. We also envision that by elaborately incorporating the multistimuli-responsive functional units into the supramolecular assembled entities, one can fabricate more sophisticated and advanced molecular materials with new functionality, good reproducibility, and easier operability.

Experimental Section

Materials

All the reagents and solvents were commercially available and used as received unless otherwise specified. 1-Methyl-4-(4-pyridyl)-pyridinium iodide, 2-hydroxyl-6-propargyloxy naphthalene, and 6-deoxy-6-azido-α-CD were synthesized according to the previous literature reports.[10] Column chromatography was performed on silica gel (200–300 mesh) and reverse-phase ODS-SM-50B (MPLC).

Measurements

NMR spectroscopic data were recorded using a 300 or 400 MHz spectrometer in D_2O or [D_6]DMSO. Mass spectra were performed using an ESI-mode MS. UV/Vis absorption spectra were recorded using a UV/Vis spectrometer (light path 10 mm). Steady-state fluorescence spectra were recorded in a conventional quartz cell (light path 10 mm) using a fluorescence spectrometer. CD spectra were collected using a spectropolarimeter in a 10 mm light-path quartz cell. The temperature was controlled using a TCU accessory with a temperature probe, which was plunged into the cuvette to measure the sample temperature. In DLS measurements, the sample solution was filtered through a 0.45 μm filter into a clean scintillation vial and then was examined using a laser-light scattering spectrometer equipped with a digital correlator at 636 nm at a scattering angle of 90°. In TEM measurements, a portion (5 μL) of the dilute aqueous solution was dropped onto a copper grid and then the grid was air-dried. The TEM samples were examined using an accelerating voltage of 200 kV. The sample for AFM measurements was prepared by dropping a portion (25 μL) of the dilute sample solution onto a newly clipped mica, and then the excess amount of aqueous solution was blotted away with a piece of filter paper 2 min later. The mica was washed with distilled water (1 mL) and then air-dried. The samples were examined in tapping mode in air at room temperature. All the microcalorimetric titration experiments were performed using a Microcal VP-ITC titration microcalorimeter, which permitted us to simultaneously determine the enthalpy change (ΔH) and the equilibrium constant (K_S) from a single titration curve. The sample cell volume was 1.4227 mL. Each titration experiment included 25 successive injections. All solutions were degassed and thermally equilibrated using a thermostat (ThermoVac accessory) before the titration experiments were performed. ORIGIN software (Microcal) was used for the calculation of binding constant (K_S) and standard molar reaction enthalpy (ΔH°) from each titration curve with a standard derivation on the basis of the scattering of data points in a single titration experiment. The binding stoichiometry (n) was also given as a fitting parameter. From the binding constant (K_S) and molar reaction enthalpy (ΔH) obtained, one can calculate the standard Gibbs free energy of binding (ΔG) and the entropy change (ΔS).

Synthesis of 2-hydroxyl-6-triazole naphthalene-modified α-CD (1)

6-Deoxy-6-azido-α-CD (473 mg, 0.46 mmol) in H_2O (10 mL) was added under stirring to a solution of 2-hydroxyl-6-propargyloxy naphthalene (90 mg, 0.45 mmol) in THF (30 mL). Then $CuSO_4 \cdot 5H_2O$ (237 mg, 0.95 mmol) and sodium ascorbate (658 mg, 2.85 mmol) dissolved in water (20 mL) were added under an Ar atmosphere. The resulting solution was heated at 60 °C for 48 h. The mixture was dried under vacuum and then dissolved in H_2O (30 mL). After the brown precipitate was removed, the filtrate was poured into acetone (500 mL). The crude product was filtered and then purified by MPLC (ethanol/water as eluent) to give the product as a colorless powder in 40% yield. ^{1}H NMR (400 MHz, D_2O): $\delta = 8.02$ (s, 1H), 7.68 (d, $J = 9.5$ Hz, 1H), 7.62 (d, $J = 8.9$ Hz, 1H), 7.34 (s, 1H), 7.09 (m, 3H), 5.27 (s, 2H), 5.02–4.80 (m, 6H), 4.60 (m, 3H), 4.07–3.11 (m, 31H), 2.94 (d, $J = 10.1$ Hz, 1H), 2.60 ppm (d, $J = 11.2$ Hz, 1H); ^{1}H NMR (400 MHz, [D_6]DMSO): $\delta = 9.48$ (s, 1H), 8.18 (s, 1H), 7.66 (d, $J = 8.6$ Hz, 1H), 7.60 (d, $J = 9.1$ Hz, 1H), 7.38 (d, $J = 2.2$ Hz, 1H), 7.13–7.01 (m, 3H), 5.65–5.42 (m, 12H), 5.18 (s, 2H), 4.85–4.77 (m, 6H), 4.61–4.44 (m, 5H), 4.08–3.47 (m, 24H), 3.31–3.14 ppm (m, overlaps with HOD); ^{13}C NMR (101 MHz, [D_6]DMSO): $\delta = 153.8$, 153.6, 151.4, 142.5, 129.9, 128.4, 128.1, 127.9, 127.5, 126.1, 122.3, 118.9, 118.8, 109.7, 108.8, 108.6, 107.4, 106.9, 101.9, 101.7, 99.5, 82.0, 77.4, 73.2, 72.4, 72.1, 71.9, 61.1, 60.8, 59.9, 49.9 ppm; ESI-MS: m/z: 1196.3982 $[M+H]^+$, 1218.3793 $[M+Na]^+$.

Synthesis of the azobenzene–bispyridinium conjugate (2)

4-(Phenyldiazenyl)phenol (990 mg, 5 mmol), potassium carbonate (4.14 g, 30 mmol), and 1,2-dibromoethane (3.74 g, 20 mmol) were dissolved in acetone (80 mL), and the mixture was heated at 60 °C for 6 h. After the precipitate was removed, the filtrate was evaporated under vacuum and then purified by silica gel column chromatography (CH_2Cl_2 as eluent) to give the product as an orange powder (**4**) in 90% yield. ^{1}H NMR (400 MHz, $CDCl_3$): $\delta = 7.93$ (d, $J = 8.8$ Hz, 2H), 7.88 (d, $J = 7.6$ Hz, 2H), 7.51 (t, $J = 7.5$ Hz, 2H), 7.46 (d, $J = 7.1$ Hz, 1H), 7.03 (d, $J = 8.8$ Hz, 2H), 4.38 (t, $J = 6.2$ Hz, 2H), 3.69 ppm (t, $J = 6.2$ Hz, 2H).

Next, 1-methyl-4-(4-pyridyl)pyridinium iodide (749 mg, 2.5 mmol) and compound **4** (763 mg, 0.2 5 mmol) were dissolved in DMF (20 mL). Then the mixture was heated to reflux for 12 h. The precipitate product was filtered and washed with CH_3CN to give the target product as a yellow powder (**2**) in 20% yield. ^{1}H NMR (400 MHz, D_2O): $\delta = 9.26$ (d, $J = 6.9$ Hz, 2H), 9.01 (d, $J = 6.5$ Hz, 2H), 8.54 (d, $J = 6.7$ Hz, 2H), 8.48 (d, $J = 6.1$ Hz, 2H), 7.83 (d, $J = 9.0$ Hz, 2H), 7.79 (d, $J = 7.8$ Hz, 2H), 7.60 (td, $J = 5.9$, 1.6 Hz, 3H), 7.15 (d, $J = 9.0$ Hz, 2H), 5.21 (t, $J = 5.3$ Hz, 2H), 4.75 (t, $J = 4.7$ Hz, 2H overlap with DOH), 4.44 ppm (s, 3H); ^{13}C NMR (101 MHz, D_2O): $\delta = 160.1$, 151.9, 150.5, 149.4, 146.8, 146.3, 146.2, 131.4, 129.6, 129.2, 126.8, 126.6, 124.5, 123.7, 122.1, 120.0, 115.4, 114.6, 66.2, 61.1, 48.3 ppm; ESI-MS: m/z: 198.0993 $[M-I-Br]^{2+}$.

Acknowledgements

This work was financially supported by the 973 Program (2011CB932502) and the National Natural Science Foundation of China (NNSFC) (91227107 and 21102075).

Keywords: cyclodextrins · host–guest chemistry · polymers · self-assembly · supramolecular chemistry

[1] a) H.-J. Kim, T. Kim, M. Lee, *Acc. Chem. Res.* **2011**, *44*, 72–82; b) X. Yan, F. Wang, B. Zheng, F. Huang, *Chem. Soc. Rev.* **2012**, *41*, 6042–6065; c) R. Chakrabarty, P. S. Mukherjee, P. J. Stang, *Chem. Rev.* **2011**, *111*, 6810–6918; d) T. Fenske, H.-G. Korth, A. Mohr, C. Schmuck, *Chem. Eur. J.* **2012**, *18*, 738–755.

[2] a) L. Fang, M. Hmadeh, J. Wu, M. A. Olson, J. M. Spruell, A. Trabolsi, Y.-W. Yang, M. Elhabiri, A.-M. Albrecht-Gary, J. F. Stoddart, *J. Am. Chem. Soc.* **2009**, *131*, 7126–7134; b) C. Park, K. Oh, S. C. Lee, C. Kim, *Angew. Chem. Int. Ed.* **2007**, *46*, 1455–1457; *Angew. Chem.* **2007**, *119*, 1477–1479; c) Y. K. Joung, T. Ooya, M. Yamaguchi, N. Yui, *Adv. Mater.* **2007**, *19*, 396–400.

[3] a) M. Ikeda, R. Ochi, Y.-s. Kurita, D. J. Pochan, I. Hamachi, *Chem. Eur. J.* **2012**, *18*, 13091–13096; b) J. Wang, P. Gao, L. Ye, A.-y. Zhang, Z.-g. Feng, *Polym. Chem.* **2011**, *2*, 931–940.

[4] a) S. Yagai, A. Kitamura, *Chem. Soc. Rev.* **2008**, *37*, 1520–1529; b) S. Saha, J. F. Stoddart, *Chem. Soc. Rev.* **2007**, *36*, 77–92; c) S. Saha, E. Johansson, A. H. Flood, H. R. Tseng, J. I. Zink, J. F. Stoddart, *Chem. Eur. J.* **2005**, *11*, 6846–6858; d) L. Zhu, H. Yan, X.-J. Wang, Y. Zhao, *J. Org. Chem.* **2012**, *77*, 10168–10175.

[5] a) M. Nakahata, Y. Takashima, H. Yamaguchi, A. Harada, *Nat. Commun.* **2011**, *2*, 511–516; b) D.-S. Guo, S. Chen, H. Qian, H.-Q. Zhang, Y. Liu, *Chem. Commun.* **2010**, *46*, 2620–2622; c) S. Saha, A. H. Flood, J. F. Stoddart, S. Impellizzeri, S. Silvi, M. Venturi, A. Credi, *J. Am. Chem. Soc.* **2007**, *129*, 12159–12171.

[6] a) B. Zheng, F. Wang, S. Dong, F. Huang, *Chem. Soc. Rev.* **2012**, *41*, 1621–1636; b) T. F. A. De Greef, M. M. J. Smulders, M. Wolffs, A. P. H. J. Schenning, R. P. Sijbesma, E. W. Meijer, *Chem. Rev.* **2009**, *109*, 5687–5754; c) L. Brunsveld, B. J. B. Folmer, E. W. Meijer, R. P. Sijbesma, *Chem. Rev.* **2001**, *101*, 4071–4097.

[7] a) Y. Zhou, L.-L. Tan, Q.-L. Li, X.-L. Qiu, A.-D. Qi, Y. Tao, Y.-W. Yang, *Chem. Eur. J.* **2014**, *20*, 2998–3004; b) C. Ke, N. L. Strutt, H. Li, X. Hou, K. J. Hartlieb, P. R. McGonigal, Z. Ma, J. Iehl, C. L. Stern, C. Cheng, Z. Zhu, N. A. Vermeulen, T. J. Meade, Y. Y. Botros, J. F. Stoddart, *J. Am. Chem. Soc.* **2013**, *135*, 17019–17030; c) R. Sun, C. Xue, X. Ma, M. Gao, H. Tian, Q. Li, *J. Am. Chem. Soc.* **2013**, *135*, 5990–5993; d) Y. Chen, Y.-M. Zhang, Y. Liu, *Isr. J. Chem.* **2011**, *51*, 515–524; e) Y. Liu, C.-F. Ke, H.-Y. Zhang, W.-J. Wu, J. Shi, *J. Org. Chem.* **2006**, *71*, 280–283.

[8] Z. Huang, L. Yang, Y. Liu, Z. Wang, O. A. Scherman, X. Zhang, *Angew. Chem. Int. Ed.* **2014**, *53*, 5351–5355; *Angew. Chem.* **2014**, *126*, 5455–5459.

[9] a) X. Ma, H. Tian, *Acc. Chem. Res.* **2014**, *47*, 1971–1981; b) X. Yao, T. Li, S. Wang, X. Ma, H. Tian, *Chem. Commun.* **2014**, *50*, 7166–7168; c) Q. Zhang, D.-H. Qu, X. Ma, H. Tian, *Chem. Commun.* **2013**, *49*, 9800–9802; d) Q. Zhang, X. Yao, D.-H. Qu, X. Ma, *Chem. Commun.* **2014**, *50*, 1567–1569; e) X. Yao, X. Ma, H. Tian, *J. Mater. Chem. C* **2014**, *2*, 5155–5160.

[10] a) L. Li, H.-Y. Zhang, J. Zhao, N. Li, Y. Liu, *Chem. Eur. J.* **2013**, *19*, 6498–6506; b) Y. Liu, C.-F. Ke, H.-Y. Zhang, J. Cui, F. Ding, *J. Am. Chem. Soc.* **2007**, *129*, 600–605.

[11] a) W. S. Jeon, E. Kim, Y. H. Ko, I. Hwang, J. W. Lee, S.-Y. Kim, H.-J. Kim, K. Kim, *Angew. Chem. Int. Ed.* **2005**, *44*, 87–91; *Angew. Chem.* **2005**, *117*, 89–93; b) Z.-J. Ding, H.-Y. Zhang, L.-H. Wang, F. Ding, Y. Liu, *Org. Lett.* **2011**, *13*, 856–859.

[12] Y. Wang, N. Ma, Z. Wang, X. Zhang, *Angew. Chem. Int. Ed.* **2007**, *46*, 2823–2826; *Angew. Chem.* **2007**, *119*, 2881–2884.

[13] H.-J. Kim, J. Heo, W. S. Jeon, E. Lee, J. Kim, S. Sakamoto, K. Yamaguchi, K. Kim, *Angew. Chem. Int. Ed.* **2001**, *40*, 1526–1529; *Angew. Chem.* **2001**, *113*, 1574–1577.

[14] a) S. Di Motta, T. Avellini, S. Silvi, M. Venturi, X. Ma, H. Tian, A. Credi, F. Negri, *Chem. Eur. J.* **2013**, *19*, 3131–3138; b) H. Bakirci, X. Zhang, W. M. Nau, *J. Org. Chem.* **2004**, *69*, 39–46.

[15] N. Berova, K. Nakanishi, R. W. Woody, *Circular Dichroism, Principles and Applications*, 2ednd edWiley–VCH, New York, Chichester, Weinheim, Brisbane, Singapore, Toronto, **2000**.

[16] A. Coleman, I. Nicolis, N. Keller, J. Dalbiez, *J. Inclusion Phenom. Mol. Recognit. Chem.* **1992**, *13*, 139–143.

[17] a) C. Stoffelen, J. Voskuhl, P. Jonkheijm, J. Huskens, *Angew. Chem.* **2014**, *126*, 3468–3472; *Angew. Chem. Int. Ed.* **2014**, *53*, 3400–3404; b) J. del Barrio, P. N. Horton, D. Lairez, G. O. Lloyd, C. Toprakcioglu, O. A. Scherman, *J. Am. Chem. Soc.* **2013**, *135*, 11760–11763; c) F. Tian, D. Jiao, F. Biedermann, O. A. Scherman, *Nat. Commun.* **2012**, *3*, 1207–1215.

[18] a) Y. Liu, Y. Yu, J. Gao, Z. Wang, X. Zhang, *Angew. Chem. Int. Ed.* **2010**, *49*, 6576–6579; *Angew. Chem.* **2010**, *122*, 6726–6729; b) K. Kim, D. Kim, J. W. Lee, Y. H. Ko, K. Kim, *Chem. Commun.* **2004**, 848–849.

[19] E. A. Appel, F. Biedermann, U. Rauwald, S. T. Jones, J. M. Zayed, O. A. Scherman, *J. Am. Chem. Soc.* **2010**, *132*, 14251–14260.

[20] K. Moon, J. Grindstaff, D. Sobransingh, A. E. Kaifer, *Angew. Chem. Int. Ed.* **2004**, *43*, 5496–5499; *Angew. Chem.* **2004**, *116*, 5612–5615.

Received: July 2, 2014
Published online on October 3, 2014